Self-recognition in corals facilitates deep-sea habitat engineering

S. J. Hennige[1], C. L. Morrison[2], A. U. Form[3], J. Büscher[3], N. A. Kamenos[4] & J. M. Roberts[1,5,6]

[1]Centre for Marine Biodiversity and Biotechnology, Heriot-Watt University, Edinburgh, EH14 4AS, Scotland, [2]U.S. Geological Survey, Leetown Science Center, Kearneysville, WV 25430, USA, [3]GEOMAR, Helmholtz Centre for Ocean Research, Kiel, 24105, Germany, [4]School of Geographical and Earth Sciences, University of Glasgow, Glasgow, G12 8QQ, Scotland, [5]Scottish Association for Marine Science, Oban, PA37 1QA, Scotland, [6]University of North Carolina Wilmington, NC 28403, USA.

The ability of coral reefs to engineer complex three-dimensional habitats is central to their success and the rich biodiversity they support. In tropical reefs, encrusting coralline algae bind together substrates and dead coral framework to make continuous reef structures, but beyond the photic zone, the cold-water coral *Lophelia pertusa* also forms large biogenic reefs, facilitated by skeletal fusion. Skeletal fusion in tropical corals can occur in closely related or juvenile individuals as a result of non-aggressive skeletal overgrowth or allogeneic tissue fusion, but contact reactions in many species result in mortality if there is no 'self-recognition' on a broad species level. This study reveals areas of 'flawless' skeletal fusion in *Lophelia pertusa*, potentially facilitated by allogeneic tissue fusion, are identified as having small aragonitic crystals or low levels of crystal organisation, and strong molecular bonding. Regardless of the mechanism, the recognition of 'self' between adjacent *L. pertusa* colonies leads to no observable mortality, facilitates ecosystem engineering and reduces aggression-related energetic expenditure in an environment where energy conservation is crucial. The potential for self-recognition at a species level, and subsequent skeletal fusion in framework-forming cold-water corals is an important first step in understanding their significance as ecological engineers in deep-seas worldwide.

T ropical scleractinian coral reefs are largely consolidated by photosynthetic coralline algae that bind coral framework and sediment to create extensive shallow-water reef systems. However, coral reefs are not restricted to tropical waters, and reef framework forming cold-water corals are found in deep-water continental shelf, slope and seamount settings across the globe (Fig. 1). Of these corals, *Lophelia pertusa* is the most globally widespread and forms extensive carbonate framework reefs[1]. Since *Lophelia*-engineered reef systems are mostly below the photic zone, coralline algae are not available to bind the reefs together. In such cold-water coral reefs, consolidation is facilitated by skeletal fusion between individual *L. pertusa* colonies that are over several years of age (assuming annual polyp division)[2].

While it is known that *L. pertusa* branches within individual colonies routinely fuse, it is often impossible to identify where fusion has occurred between different colonies. In cases where fusion has been identified, it has been assumed that both colonies were closely related, and were displaying characteristics which have also been noted in tropical corals[3–5].

True skeletal fusion in tropical corals occurs in conjunction with allogeneic tissue fusion, which is controlled by allorecognition, a major characteristic in invertebrate immunity[4] that depends upon the ability to recognise self and non-self[4,6]. In tropical corals, the ability to allorecognise depends largely on the maturity of the individuals with allogeneic fusion only reported in juvenile corals. In tropical corals it is thought that the lack of an active historecognition system during the early stages of ontogeny (4–8 months) allows juveniles of the same species to occasionally allogeneically fuse[6–8]. However, allorecognition in corals is a complex synergy of effector mechanisms, specificity and competency[4,6,9], which may have evolved as far back as 400 million years ago[10]. Allogeneic interactions between juvenile tropical corals fall into three groups: (A) true fusion (resulting in a chimaera), (B) incompatible fusion, or (C) non-fusion[6]. True fusion will often be followed by incompatible fusion, when one colony reaches historecognition maturity or starts to discriminate between self and non-self. At this point, skeletal ridges or overgrowth may occur but, importantly, continuous framework will have been established between colonies[8].

This study examines the ability of *L. pertusa* to achieve skeletal fusion between genetically distinct individuals. If genetically distinct *L. pertusa* colonies reacted aggressively when they came into contact, as is the case for some adult genetically distinct tropical corals[3,11], the reef frameworks built by this species would not be as large or as
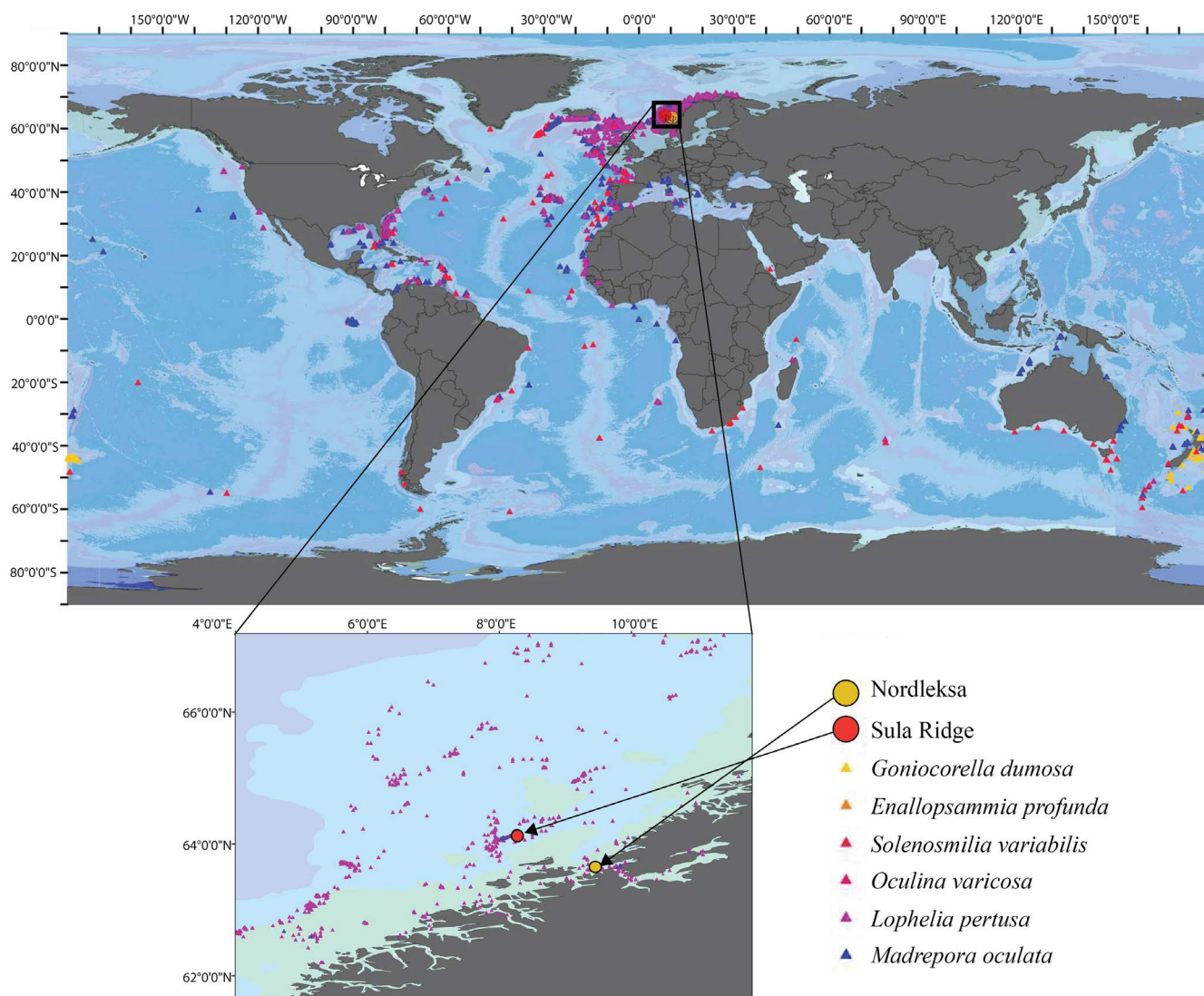
Figure 1 | **Global framework-forming cold-water coral distribution map based on data in Freiwald et al.[23], and location of two Norwegian study sites.** Map made using ArcMAP 9.3.

stable given the absence of encrusting coralline algae. The skeletal fusion reported for the first time in this study is either the result of allogeneic fusion followed by incompatible fusion, or efficient, low aggression overgrowth of one individual into another as a result of self-recognition on a species level[3]. The low aggression between individuals is apparent by the visible lack of a 'dead-zone' where no tissue covers the skeleton, or a very small area (<1 mm), as opposed to the larger dead zones that are noted following tropical coral contact reactions[3,11]. This could indicate either a lack of aggression or a reduced form of aggression compared to tropical corals. Regardless of whether allogeneic fusion or low-aggression efficient overgrowth is most prevalent, or whether both occur, the degree of observed skeletal fusion on *L. pertusa* reefs[12] highlights how self-recognition on a species level underpins the success of this key ecosystem engineer.

Results

Several skeletal fusion instances were observed in adult *L. pertusa* colonies (Fig. 2A). Ridges and skeletal overgrowth is apparent in Fig. 2A and B, where an orange polyp has been encased by white skeleton. Where multiple contact events between two polyps are observed (Fig. 2C), possible reversal of overgrowth is observed, as orange tissue re-grew over white skeleton. The dominant coral in this

case through non-transitive hierarchy is not clear, which is consistent with observations that white and orange colonies of *L. pertusa* remain distinct (i.e. separate individuals) beyond their sites of initial and continued fusion (Fig. 2D). If one colony was 'dominant', it could be expected that a large proportion of overgrowth by that colony would occur as a result of dominant aggression.

Physical structure. Cross-sectional SEM imaging of a fusion contact zone reveals instances where there is no clear demarcation of one polyp ending and another beginning, indicating full skeletal fusion (Fig. 3A–D). However, a 'micro-suture' between the orange and white polyp (Fig. 3E, F) ranging from <1 to 3 μm is visible in parts of the sample. The orange polyp has a highly organised crystallographic structure near the micro-suture (Fig. 3F, using Electron Back Scatter Diffraction (EBSD)). In contrast, the white polyp appears to either have crystals too small for visualisation, or a high organic content (e.g. Cusack et al.[13]). While individual crystal orientation may change depending upon the cross-section location, the lack of crystallographic organisation in the white polyp compared to the orange polyp (Fig. 3E, F) differs to crystallographic organisation in non-fused white *L. pertusa* polyp examples (see Fig. S1), where large, well-organised aragonite crystals are identifiable in a variety of orientations. Cavities were also identified near fusion

Figure 2 | Skeletal fusion events between white and orange colonies of the cold-water coral *Lophelia pertusa* from Nordleksa reef, Norway, ~150 m depth, observed September 2011. (A) Multiple fusion events between two colonies. The box on the right is cross-sectioned in Fig. 3. (B) An example of an orange polyp overgrown by a white skeleton. Arrows indicate orange coenosarc now growing on white skeleton. (C) Two separate skeletal fusion events between an adult white and orange polyp. (D) Orange and white colonies coming into contact and fusing on Norwegian reefs. (A–C) permission of Solvin Zankl. (D) Permission of JAGO-Team, GEOMAR.

zones and in both polyps, where crystals appear to originate from different centres of calcification. Micro-sutures also originate from these holes, with diffraction and crystallographic orientation indicating that aragonite crystals interlocked successfully (Fig. 4A–C).

Molecular structure. Changes in the physical structure of the skeleton at the different fusion zones were identified by using Raman spectroscopy. A decrease in the width (Full Width Half Maximum, FWHM) of the ca. 1085 cm^{-1} peak indicates decreased calcium carbonate bond lengths[15]. These shorter bond lengths are stronger, but are the result of greater molecular disorder[14,15]. Where no micro-suture was identified between the white and orange polyps (Fig. 3C), the FWHM was significantly smaller than the FWHM of the white polyp where a large (ca. 2 μm) micro-suture was evident (Mann-Whitney U = 0.00, p = 0.036, d.f. = 6) (Fig. 5B), but not significantly smaller than the orange polyp. FWHMs (n = 3) of both

polyps at the small micro-suture (<1 μm) were smaller than at a large suture, but this difference was not significant. FWHM on both polyps on the opposite side to fusion events were markedly different from each other (Fig. 5C). To account for variability in FWHM being potentially caused by crystal size, orientation, and potential organic content, transects were taken at fusion areas (Fig. 5A, S1). The differences described above, where FWHM was lower at the sutureless zone compared to suture zones were still observed as distance away from the suture increased, and hence represented biologically controlled differences, and not artefacts of the cross-section location.

Genetic relatedness. Maximum-likelihood estimates of relatedness (*r*) were generated from multi-locus genotypes, including 15 microsatellite markers, for *L. pertusa* individuals from Nordleksa and Sula Ridge sites. Relatedness estimates ranged from 0.00 (unrelated, 148 of 182 pairwise comparisons) to 0.66 (full siblings,
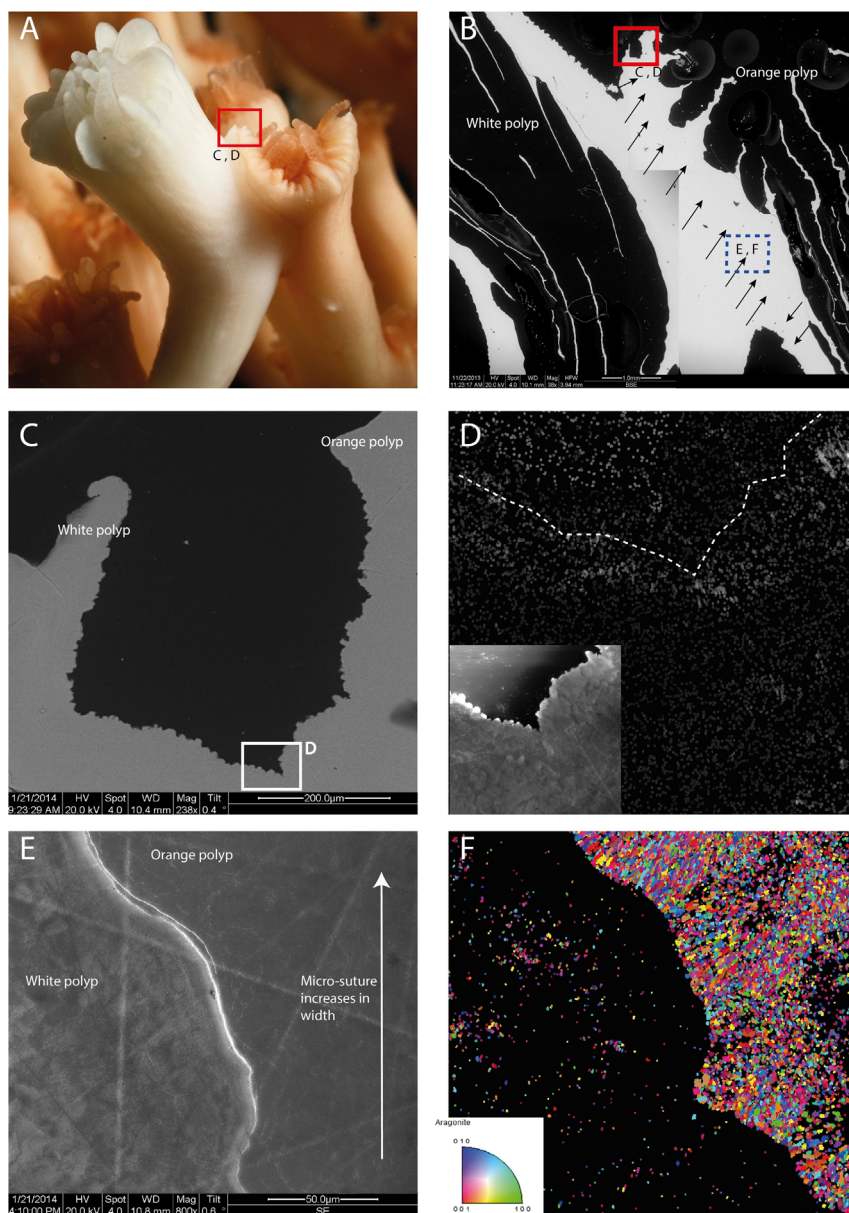
Figure 3 | (A) Close-up image of a skeletal fusion-zone between white and orange *Lophelia pertusa* polyps. Note the occurrence of live, potentially allogeneically fused tissue within the red box. (B) Back Scattered Electron emission (BSE) micrograph of skeletal fusion between white and orange individual polyps of *L. pertusa* pictured in (A). The dashed box represents an identified 'micro-suture' between the polyps (expanded in (E) and (F)), and arrows indicate the proposed area of fusion between the two polyps. (C) BSE micrograph of fused area depicted in (A and B). No suture was identified, and a likely area of fusion was enlarged in (D) for diffraction intensity analysis of aragonite crystals (crystals are the defined white areas). (D) is secondary electron (SE) micrograph of same area. (E, F) enlarged area of identified micro-suture (SE micrograph) and corresponding crystallographic orientation of aragonite respectively. Colours in (F) indicate crystal orientation. (A) permission of Solvin Zankl.

4 Sula Ridge comparisons), with 3 Sula Ridge comparisons estimated to be half-sibs ($r = 0.32$) (Table 1). The two fused individuals were classified as unrelated in the analysis ($r = 0.00$), and the probability that these individuals were unrelated did not change when the frequencies of null alleles were included.

Discussion

The ability of *L. pertusa* to skeletally fuse[12] between individuals has facilitated their roles as deep-sea ecosystem engineers. Here we demonstrate that this can occur between genetically distinct adult individuals and not just between closely related individuals. It is likely that this ability has been driven by two main factors: 1) evolutionary pressure for cold-water corals to stabilise their own framework, much like the role of calcifying encrusting algae on tropical reefs,

and 2) the benefit of reducing energetic investment into aggressive competition interactions, which can lead to mortality or reductions in growth and gonad development in reef forming corals[11]. Creation of continuous reef frameworks would ensure suitable substrate is formed for the settlement of subsequent generations providing a selective advantage. Skeletal fusion would also act to prevent unnecessary coral death if the underlying framework is broken e.g. from strong currents and/or bioerosion, as live coral branches falling into other colonies would be more likely to survive and grow. Since deep-water corals rely purely on heterotrophic feeding (i.e. feeding on passing prey items, which varies spatially and temporally) avoiding unnecessary energetic expenditure, which could be reallocated to growth and reproduction, would be of significant benefit to the success and continuation of *L. pertusa* reefs.
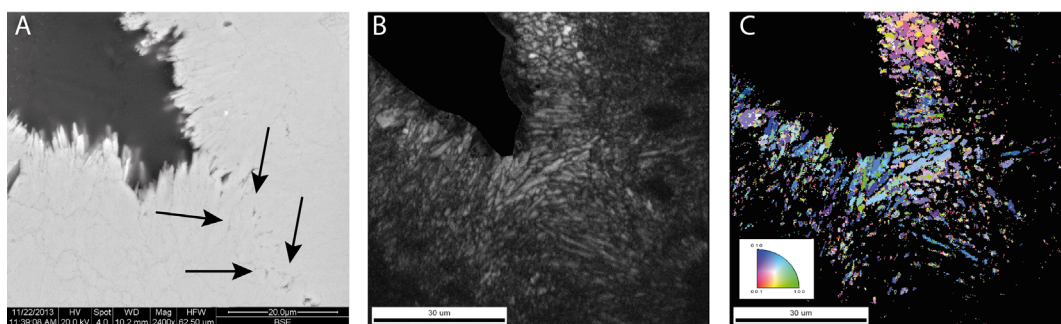
Figure 4 | Back Scattered Electron emission (BSE), diffraction intensity and Electron Back Scatter Diffraction (EBSD) of a cavity observed near a fusion zone. (A) BSE micrograph of cavity edge with arrows indicating aragonite crystals interlocking. (B and C) Diffraction intensity map and crystallographic orientation of aragonite respectively. Colours in (C) indicate crystal orientation.

Further work is needed to identify whether this skeletal fusion is driven by: 1) allogeneic fusion between individuals, or 2) an efficient, minimally aggressive 'overgrowth' strategy across individuals that does not result in mortality of any polyps. Both of these mechanisms are represented here, and both rely on a high degree of self-recognition at a species level. Efficient overgrowth with no observable mortality is apparent in Fig. 2B and C, and potential allogeneic tissue fusion is identifiable in Fig. 3A, leading to seamless skeletal fusion (Fig. 3.D). The skeletal fusion reported here between genetically distinct individuals with unique multi-locus genotypes at 15 microsatellite loci, underpins the fact that while *L. pertusa* can discriminate 'self' on a species level, they do not reject between individuals. The occurrence of both overgrowth and potential allogeneic fusion in data presented here complements observations that allogeneic fusion is complex, and can happen in a series of cascading events[6]. For the rare instances that adult allogeneic fusion has been noted in tropical corals[16], they are typically explained by a close genetic similarity of the colonies involved[4,5].

The difference between overgrowth and tissue allogeneic fusion may be represented in: 1) the strength or molecular organisation of the aragonite bonds[14,15], and 2) the organisation or size of aragonite crystals. For 1) the decreased FWHM at the suture-less fusion zone indicates decreased molecular organisation but stronger bonding within the aragonite. FWHM in areas with small micro-sutures and larger micro-sutures increased respectively. It seems that full skeletal fusion where no suture is formed, results in strong molecular bonding, and potentially small, or disorganised crystal bundles compared to areas where sutures were apparent. Allogeneically fused tissue could thus result in different biomineralisation properties of the coral skeleton. In areas that may be the result of overgrowth, decreased aragonite bond strength of one or both of the polyps, or increased crystallographic organisation is observed. It is unknown
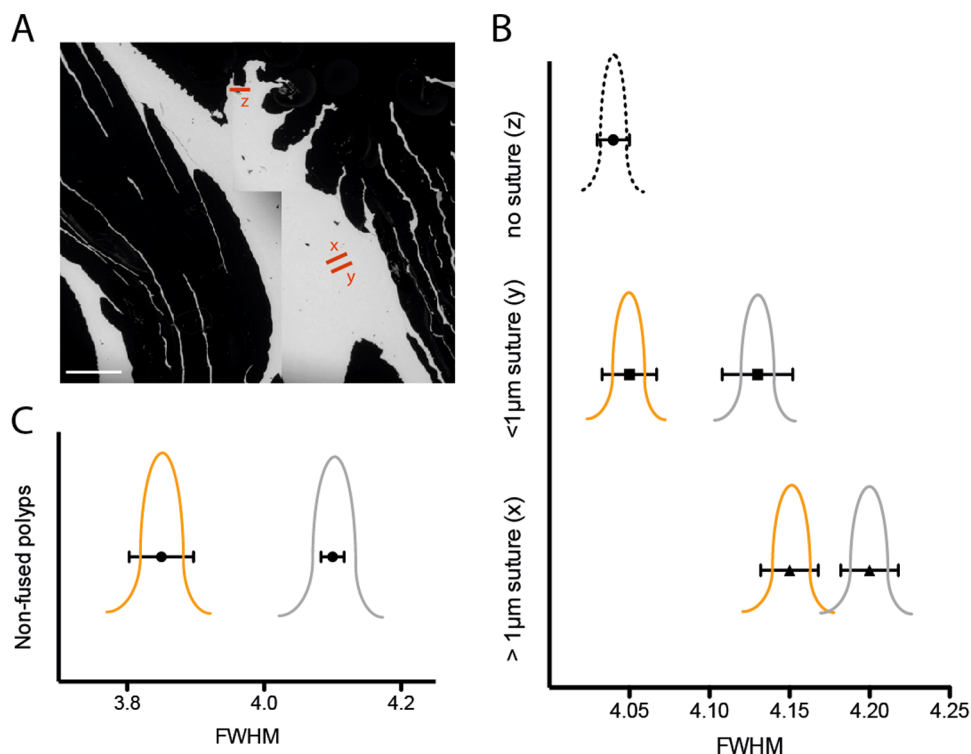

Figure 5 | (A) Back Scatter Electron emission (BSE) micrograph of Raman spectroscopy zones, scale bar 1 mm. (B) Full Width Half Maximum (FWHM) data from aragonite peak spectra at ca. 1085 cm^{-1}. X and Y data represent replicates (n = 3 ± SEM) of measurements 5 μm from the fusion point at a small (<1 μm) or relatively large (ca. 2 μm) micro-suture. Polyp identity is denoted by spectra colour (orange or grey). The dashed spectrum represents the mean area between the white and orange polyp where no micro-suture was present. (C) FWHM (n = 3 ± SEM) of aragonite peak spectra at ca. 1085 cm^{-1} of white and orange polyps on polyp sides not involved in fusion. Full transects are detailed in supplementary Fig. S1.

Table 1 | Matrix of maximum likelihood relationships between *Lophelia pertusa* individuals

	N1	N2	N3	N4	N5	N-O	N-W	S1	S2	S3	S4	S5	S6	S7
N1	1													
N2	0.00	1												
N3	0.00	0.00	1											
N4	0.00	0.00	0.0	1										
N5	0.00	0.00	0.00	0.00	1									
N-O	0.00	0.00	0.04	0.00	0.00	1								
N-W	0.00	0.00	0.00	0.00	0.00	0.00	1							
S1	0.00	0.00	0.00	0.00	0.00	0.00	0.00	1						
S2	0.09	0.03	0.00	0.00	0.00	0.00	0.00	0.15	1					
S3	0.00	0.00	0.00	0.00	0.00	0.05	0.00	0.48	0.29	1				
S4	0.00	0.00	0.00	0.00	0.00	0.00	0.00	0.61	0.26	0.66	1			
S5	0.00	0.00	0.00	0.00	0.00	0.00	0.00	0.00	0.00	0.00	0.00	1		
S6	0.00	0.00	0.00	0.00	0.00	0.00	0.00	0.00	0.00	0.00	0.00	0.66	1	
S7	0.00	0.06	0.00	0.00	0.00	0.00	0.04	0.00	0.01	0.32	0.00	0.00	0.08	1

Nordleksa (N), Sula Ridge (S) and fused orange (O) and white (W) sample. No shading represents unrelated individuals ($r \sim 0.00$) (Yellow is the highlighted orange/white fused sample); Pink indicates half siblings ($r \sim 0.25$); Blue indicates full siblings ($r \sim 0.5$). Clones or twins would be a maximum likelihood of relationship of $r = 1.00$.

how these factors are controlled when contact does occur between corals, and whether the cavities that are observed near the fusion zones are a result of fusion-skeletal effectors, or the result of overgrowth of organic debris while the coral was growing.

Aside from the specific mechanisms that facilitate this skeletal fusion, it is also unknown whether this ability is limited to the deep-water coral *L. pertusa* or whether other deep-water reef framework-forming species (see Fig. 1) also exhibit skeletal, and potential allogeneic fusion, between non-kin adult individuals. Regardless of whether the large, multi-colony frameworks which are often characteristic of *L. pertusa* reefs are mostly a result of allogeneic tissue fusion or efficient low aggression overgrowth, the ability of *L. pertusa* to self-recognise at a species level to routinely undergo skeletal fusion has made them one of the most significant ecosystem engineers of the deep seas.

Methods

The fused orange and white *L. pertusa* colony, and additional orange and white *L. pertusa* genetic material from Nordleksa reef and Sula ridge (Fig. 1) were first observed from and then collected using the two-man submersible JAGO (GEOMAR, Kiel, Germany) in September 2011. To record observations through HD video and still images, LED Multi-Sealite Matrix (DeepSea Power and Light) lights, a Sony HVR-V1E (HDV1080i) video camera, and a custom-housed GoPro HD Hero 3 camera were used. Genetic subsamples from the fused corals and neighbouring colonies were collected and stored using FTA cards (Whatman).

Total DNA was isolated from *L. pertusa* tissue preserved on the cards using the tissue protocol from the PureGene DNA extraction kit (Gentra Systems, Inc., Minneapolis, Minnesota). PCR conditions for the amplification of *L. pertusa* microsatellite loci followed Morrison et al.[17]. Fluorescent DNA fragments were multiplexed and analysed on an ABI 3130XL Genetic Analyzer (Applied Biosystems) with Genescan-500 LIZ size standard. Genemapper fragment analysis software (Applied Biosystems) was used to score, bin and output allelic data. The program GenAlEx 6.5[18,19] provided summary statistics for the dataset including heterozygosity and alleles per locus. Genetic relatedness between individuals was estimated as the probability that individuals share zero, one or two alleles per marker that are identical by descent[20] with a maximum-likelihood based estimator in the program ML-RELATE[21]. Since the presence of null alleles can impact the accuracy of relatedness estimates[22], the presence of null alleles was tested for each locus and their frequencies estimated in ML-RELATE prior to relatedness analyses.

Characteristics of the fifteen polymorphic loci[17] to analyse relatedness are detailed in Table S1. Markers yielded between 4 and 13 alleles with an average of 9.3 alleles and a mean expected heterozygosity of 0.758 (Table S1). Deviations from Hardy-Weinberg Equilibrium were observed, with 8 out of the 15 loci showing heterozygote deficits.

To assess the biomineralisation aspects of a fused zone, the fused section pictured in Fig. 3 was set in EpoHeat epoxy (Buehler) and cross-sectioned using a slow-speed saw. The sample was polished using progressive grits (320, 1200, 2500, 4000), micropolished using alpha aluminium oxide at 1 and 0.3 μm, and then fine-polished with 0.06 μm amorphous colloidal silica (Buehler) on a short nap to remove any residual damaged surface layers[13]. Back scatter electron micrographs of the entire cross section, and likely points of fusion were then taken using an FEI Quanta 200F field emission scanning electron microscope (SEM) equipped with a TSL EBSD system and OIM version 6 at the University of Glasgow.

Grain CI tolerance was 5 with a minimum grain size of 2 pixels, neighbour CI correlation was CI 0.05. The Kikuchi patterns were indexed using the OIM Data Collection database, which contains structure files of aragonite. OIM maps were subject to two clean-up algorithm procedures to ensure reliable data were displayed, where grain CI standardization was applied with a grain tolerance angle of 5, minimum grain size of 2 pixels, and neighbour CI correlation of CI 0.2. Further partitioning of data was applied with only grains of CI Fit and displayed in the resultant OIM map to remove any background noise from the final dataset as in Cusack et al.[13].

To assess the molecular properties of the skeleton, Raman spectroscopy was used as described by Kamenos et al.[14]. The aragonite peak in *L. pertusa* is centred at ca. 1085 cm^{-1}. Raman data were collected along transects (3 replicates) along zones of interest in the sample. This included: 1) the area directly below where the samples are fused at their uppermost point, 2) zones where the micro-suture is relatively large (>1 μm) and small (<1 μm), and 3), zones on both polyps which were not involved in fusion. The full width at half maximum (FWHM) of the ca. 1085 cm^{-1} is related to positional disorder of the lattice and in turn molecular bond strength[15]. Increases in molecular bond strength can be attributed to positional disorder of crystal lattice via ions moving out of the plane parallel to the a-axis in the direction of the c-axis[15].

1. Roberts, J. M., Wheeler, A. J. & Freiwald, A. Reefs of the deep: the biology and geology of cold-water coral ecosystems. *Science* **312**, 543–547 (2006).
2. Gass, S. E. & Roberts, J. M. Growth and branching patterns of *Lophelia pertusa* (Scleractinia) from the North Sea. *J. Mar. Biol. Assoc. U. K.* **91**, 831–835 (2011).
3. Rinkevich, B. & Loya, Y. Intraspecific competitive networks in the Red Sea *coral Stylophora pistillata*. *Coral Reefs* **1**, 161–172 (1983).
4. Amar, K.-O. & Rinkevich, B. Mounting of erratic histoincompatible responses in hermatypic corals: a multi-year interval comparison. *J. Exp. Biol.* **213**, 535–540 (2010).
5. Puill-Stephan, E., Willis, B. L., van Herwerden, L. & van Oppen, M. J. H. Chimerism in wild adult populations of the broadcast spawning coral *Acropora millepora* on the Great Barrier Reef. *PLoS One* **4**, 7751 (2009).
6. Rinkevich, B. Allorecognition and xenorecognition in reef corals: a decade of interactions. *Hydrobiologia* **530/531**, 443–450 (2004).
7. Nozawa, Y. & Loya, Y. Genetic relationship and maturity state of the allorecognition system affect contact reactions in juvenile *Seriatopora* corals. *Mar. Ecol. Prog. Ser.* **286**, 115–123 (2005).
8. Hidaka, M., Yurugi, K., Sunagawa, S. & Kinzie Iii, R. A. Contact reactions between young colonies of the coral *Pocillopora damicornis*. *Coral Reefs* **16**, 13–20 (1997).
9. Rinkevich, B. The "Immunology trap" of anthozoans. *Invertebr. Surviv. J.* **8**, 153–161 (2011).
10. Noble, J. P. A. & Lee, D.-J. First report of allogeneic fusion and allorecognition in tabulate corals. *J. Paleontol.* **65**, 69–74 (1991).
11. Rinkevich, B. & Loya, Y. Intraspecific competition in a reef coral: effects on growth and reproduction. *Oecologia* **66**, 100–105 (1985).
12. Stetson, T. R., Squires, D. F. & Pratt, R. M. Coral banks occurring in deep water on the Blake Plateau. *Am. Mus. Novit.* **2114** (1962).
13. Cusack, M. *et al.* Electron backscatter diffraction (EBSD) as a tool for detection of coral diagenesis. *Coral reefs* **27**, 905–911 (2008).
14. Kamenos, N. A. *et al.* Coralline algal structure is more sensitive to rate, rather than the magnitude, of ocean acidification. *Glob. Chang. Biol.* **19**, 3621–3628 (2013).
15. Bischoff, W. D., Sharma, S. K. & Mackenzie, F. T. Carbonate ion disorder in synthetic and biogenic magnesium calcites: a Raman spectral study. *Am. Mineral.* **70**, 581–589 (1985).

16. Nozawa, Y. & Hirose, M. When does the window close? The onset of allogeneic fusion 2–3 years post-settlement in the scleractinian coral, *Echinophyllia aspera*. *Zool. Stud.* **50**, 396 (2011).

17. Morrison, C. L., Eackles, M. S., Johnson, R. L. & King, T. L. Characterization of 13 microsatellite loci for the deep-sea coral, *Lophelia pertusa* (Linnaeus 1758), from the western North Atlantic Ocean and Gulf of Mexico. *Mol. Ecol. Resour.* **8**, 1037–1039 (2008).

18. Peakall, R. O. D. & Smouse, P. E. GENALEX 6: genetic analysis in Excel. Population genetic software for teaching and research. *Mol. Ecol. Notes* **6**, 288–295 (2006).

19. Peakall, R. & Smouse, P. E. GenAlEx 6.5: genetic analysis in Excel. Population genetic software for teaching and research—an update. *Bioinformatics* **28**, 2537–2539 (2012).

20. Blouin, M. S. DNA-based methods for pedigree reconstruction and kinship analysis in natural populations. *Trends Ecol. Evol.* **18**, 503–511 (2003).

21. Kalinowski, S. T., Wagner, A. P. & Taper, M. L. ml-relate: a computer program for maximum likelihood estimation of relatedness and relationship. *Mol. Ecol. Notes* **6**, 576–579 (2006).

22. Wagner, A. P., Creel, S. & Kalinowski, S. T. Estimating relatedness and relationships using microsatellite loci with null alleles. *Heredity* **97**, 336–345 (2006).

23. Freiwald, A., Rogers, A. & Hall-Spencer, J. Global distribution of cold-water corals (version 2). UNEP World Conservation Monitoring Centre. (2005). URL: data.unep-wcmc.org/datasets/1; www.unep-wcmc.org Date accessed: 21.08.2013.

Acknowledgments

Author contributions

S.J.H. and J.M.R. jointly conceived the concept for this paper, and developed it with A.U.F., J.B., C.L.M. and N.A.K. Genetic and statistical analyses were performed by C.L.M. All authors discussed the results and context of the manuscript.

Additional information

Supplementary information accompanies this paper at http://www.nature.com/scientificreports

How to cite this article: Hennige, S.J. *et al.* Self-recognition in corals facilitates deep-sea habitat engineering. *Sci. Rep.* **4**, 6782; DOI:10.1038/srep06782 (2014).